ISSN: 2307-7743
www.scienceasia.asia

Asian J. Math. Appl. (2022) 2022:16

Coriolis Effect on MHD Hybrid Nanofluid Couette Flow Over an Exponentially Stretching Plate

W. N. Mutuku[1]

[1]Department of Mathematics and Actuarial Science, Kenyatta University, Nairobi, Kenya

Correspondence should be addressed to W. N. Mutuku: mutuku.winifred@ku.ac.ke

Abstract
The revolutionary impact of nanofluids on the advancement of technology and industrial applications can not be overlooked. Applications of nanofluid ranges from the cooling system of laptops and smartphones to the cooling system in ultra-large industrial equipments. It has been shown that hybrid nanofluids possess superior properties compared to the nanofluid themselves. In this study, the flow of hybrid nanofluid over a rotating and exponentially stretching surface is considered in the presence of a magnetic field. The equations governing the flow are formulated then transformed into dimensionless forms using appropriate similarity transformations before been solved numerically in MATLAB. The results show that Coriolis force increases primary velocity, temperature and the concentration but reduces secondary velocity. It is also noted that, movement of the upper plate increases the secondary velocity in the boundary layer but reduces the temperature and concentration.

Keywords: Hybrid nanofluid, MHD, Couette flow, Exponentially stretching surface, Coriolis force, Stretching ratio.

Background Information

Nanofluids are fluids suspending nanometre-sized particles. They were first proposed in [1] as a way to enhance the thermal and electrical properties of fluids. This class of fluids have gained attention from scientists partly because of the advancement in the nanotechnology and mostly because of the inherent potentials of its applications. Nanofluids have been applied in industries and technology to enhance cooling system in electronic gadgets, smart equipments and ultra large machines. Meanwhile, despite the numerous applications of nanofluid, a more efficient fluid called hybrid nanofluid was studied by [2]. In their experiment, Alumina and copper nanoparticles were suspended in water. The results shows that such fluid posses superior thermal properties compared with the individual nanofluids. Stretching plates have been found to be very useful in the preparation of thermal paths and thermal insulators in many practical applications. [3] studied the magnetohydrodynamic flow of Williamson fluid across a stretching plate. The flow settings include the presence of thermal radiation. [4] considered the magnetohydrodynamic flow of Eyring-Powell flow over a stretching plate with Newtonian heating. The flow identified that viscous dissipation enhances flow velocity. [5] proposed a modified version of Eyring-Powell fluid that delineates the shear thickening from the shear thinning properties of Eyring-Powell fluid. The study shows that raising the magnetic field strength during the flow of MEP fluid decelerates the velocity profiles while boosting the temperature profile.

Received: 2022-07-12

Centripetal force, centrifugal force, Euler force, Azimuthal force and Coriolis force are the inertia forces that arise in rotating frame. The rotation requires these forces to keep the motion going. The effect of Coriolis force has been found to be significant in many natural processes. Climate change, arrangement of earth's electric column, direction of tropical cyclones and true direction of sunlight can only be properly understood if Coriolis force is understood well [6]. The Coriolis force has been found to contribute significantly to the flow of fluid in a rotating frame [7]. [8] studied the flow of Newtonian fluid over a rotating nonuniform surface. The flow is set up in a magnetic field and the results indicated increasing the Coriolis force increases the flow temperature, skin friction and heat transfer rate. In the study conducted by [9], the flow of nanofluid over a rotating surface was considered. The flow is subjected to Cattaneo-Christov heat transfer. More recently, [10] studied the flow of Williamson fluid over an inclined rotating surface. A magnetic field is applied perpendicular to the inclined plane. The study analysed the effect inclination angle, magnetic strength and Coriolis force. It is concluded from the work that Coriolis force boosts heat and mass transfer in the flow.

In this study, a flow is set up between two exponentially stretching plates, where the upper and the lower plates move at different or the same exponential rates. A magnetic field that acts normal to the upper plate while the entire system rotates anticlockwise. This study investigates the effect of Coriolis force and stretching ratio on the flow. This study answers the following question;

1. How does Coriolis force the flow velocities in different directions?
2. How does Coriolis force the flow temperature in different directions?
3. How does the movement of the upper and lower plates affect the flow velocities in different directions?
4. How does the movement of the upper and lower plates affect the flow temperature and concentration?

Governing Equations

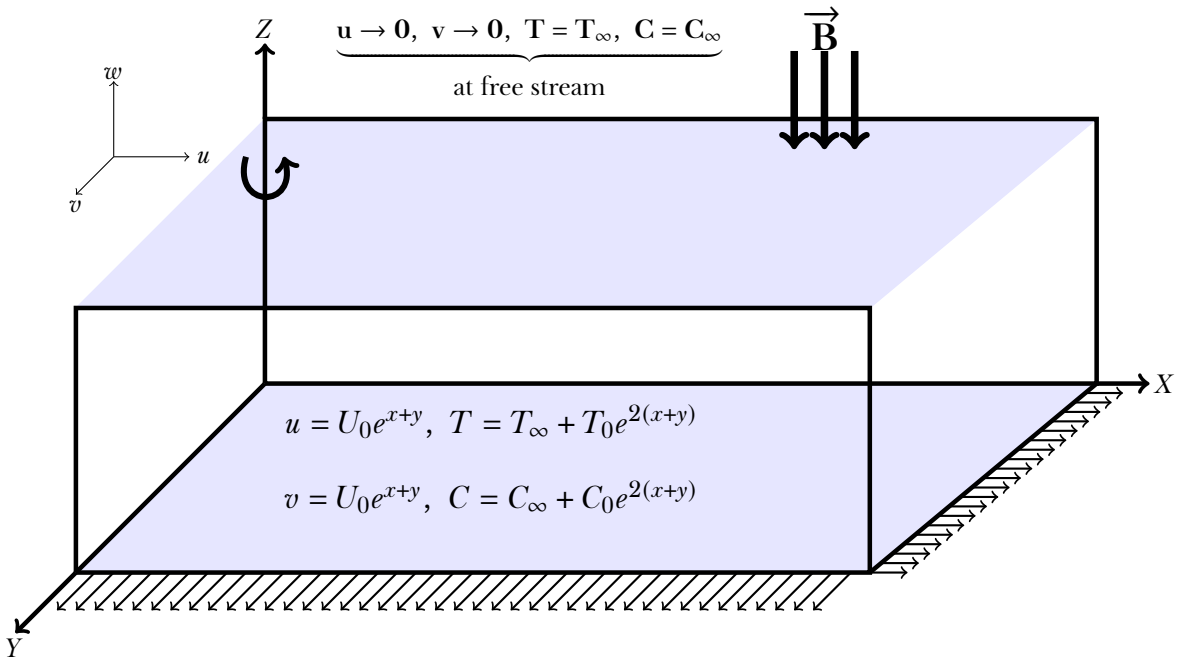

Figure 1: Flow configuration

The flow of Ethylene-Glycol in which Copper and Alumina nanoparticles are suspended is considered between two moving plates. A magnetic field of constant strength is applied normal to the upper plate and the flow regime is shown in figure (1). The primary direction is taken along the x-axis an while the secondary direction is taken along the y-axis. The surface rotates anticlockwise at a an angular speed of Ω. Coriolis force is generated due to the rotation of the surface and the flow is affected by the direction of rotation. Following the formulation of [11], the governing equations for this flow is;

$$\frac{\partial u}{\partial x}+\frac{\partial v}{\partial y}+\frac{\partial w}{\partial z}=0, \tag{1}$$

$$u\frac{\partial u}{\partial x}+v\frac{\partial u}{\partial y}+w\frac{\partial u}{\partial z}=\frac{\mu_{hnf}}{\rho_{hnf}}\frac{\partial^2 u}{\partial z^2}+g^*\beta\left(T-T_\infty\right)-\frac{\sigma_{hnf}B_0^2u}{\rho_{hnf}}+2\Omega v \tag{2}$$

$$u\frac{\partial v}{\partial x}+v\frac{\partial v}{\partial y}+w\frac{\partial v}{\partial z}=\frac{\mu_{hnf}}{\rho_{hnf}}\frac{\partial^2 v}{\partial z^2}+g^*\beta\left(T-T_\infty\right)+\frac{\sigma_{nf}B_0^2v}{\rho_{hnf}}-2\Omega u \tag{3}$$

$$u\frac{\partial T}{\partial x}+v\frac{\partial T}{\partial y}+w\frac{\partial T}{\partial z}=\left(\alpha_{hnf}+\frac{16\sigma^*T_\infty^3}{3k^*\left(\rho c_p\right)_{hnf}}\right)\frac{\partial^2 T}{\partial z^2}+\tau\left[\frac{D_B}{\Delta C}\frac{\partial C}{\partial z}\frac{\partial T}{\partial z}+\frac{D_T}{T_\infty}\frac{\partial T}{\partial z}\frac{\partial T}{\partial z}\right] \tag{4}$$

$$u\frac{\partial C}{\partial x}+v\frac{\partial C}{\partial y}+w\frac{\partial C}{\partial z}=D_B\frac{\partial^2 C}{\partial z^2}+\frac{D_T\Delta C}{T_\infty}\frac{\partial^2 T}{\partial z^2}, \tag{5}$$

The boundary conditions are

$$\text{at } z=0,\ \begin{cases} u=U_w=U_0e^{x+y},\ v=V_w=V_0e^{x+y},\ w=0, \\ T=T_w=T_\infty+T_0e^{2(x+y)}\ C=C_w=C_\infty+\Delta Ce^{2(x+y)} \end{cases} \tag{6}$$

$$\text{as } z\to\infty,\ u\to 0,\ v\to 0,\ T\to T_\infty,\ C\to C_\infty. \tag{7}$$

The effective dynamic viscosity μ_{hnf} and effective density ρ_{hnf} of the hybrid nanofluid [12] are defined as

$$\mu_{hnf}=\left(1-\phi\right)^{-2.5}\mu_{bf},\quad \rho_{hnf}=\left(1-\phi\right)\rho_{bf}+\phi_1\rho_1+\phi_2\rho_2,$$

where ϕ is the overall volume fraction defined as

$$\phi=\phi_1+\phi_2.$$

The effective thermal diffusivity α_{hnf} and the specific heat capacity $\left(\rho c_p\right)_{hnf}$ [13–15] are defined as

$$\alpha_{hnf}=\frac{k_{hnf}}{\left(\rho c_p\right)_{hnf}},\quad \frac{\left(\rho c_p\right)_{hnf}}{\left(\rho c_p\right)_{bf}}=1-\phi+\phi_1\frac{\left(\rho c_p\right)_1}{\left(\rho c_p\right)_{bf}}+\frac{\phi_2\left(\rho c_p\right)_2}{\left(\rho c_p\right)_{bf}}, \tag{8}$$

$$\frac{k_{hnf}}{k_{bf}}=\frac{\left(1+2\phi\right)\left(\phi_1k_1+\phi_2k_2\right)+2\left(1-\phi\right)\phi k_{bf}}{\left(1-\phi\right)\left(\phi_1k_1+\phi_2k_2\right)+\left(2+\phi\right)\phi k_{bf}}. \tag{9}$$

The quantities of engineering interest are the skin friction and the heat transfer rate along the x-direction and z-direction and defined as

$$Cf_x=\frac{\tau_x}{\rho_{hnf}U_w^2},\quad Cf_z=\frac{\tau_y}{\rho_{hnf}U_w^2},\quad \text{and}\quad Nu=\frac{zq_w}{\kappa_{hnf}\left(T_w-T_\infty\right)}. \tag{10}$$

respectively [16]. The shear stress (skin friction along the x and y direction) τ along the wall and the heat flux q_w at the wall are defined as [7]

$$\tau_x = \mu_{hnf} \left.\frac{\partial u}{\partial z}\right|_{z=0}, \ \tau_z = \mu_{hnf} \left.\frac{\partial v}{\partial z}\right|_{z=0}, \text{ and } q_w = -\kappa_{hnf} \left.\frac{\partial T}{\partial z}\right|_{z=0}. \tag{11}$$

Methodology

The partial differential equations (1 - 4) with the initial and boundary conditions (6 - 7) are nondimensionalised using the similarity variables

$$\eta = \left(\frac{U_0}{2\nu_{bf}}\right)^{\frac{1}{2}} z \exp\left(\frac{x+y}{2}\right), u = U_0 f'(\eta) \exp(x+y), \tag{12}$$

$$v = U_0 g'(\eta) \exp(x+y), \ T = T_\infty + \theta T_0 \exp(2x+2y), \ C = C_\infty + \Phi \Delta C \exp(2x+2y), \tag{13}$$

$$w = -\left(\frac{\nu_{bf} U_0}{2}\right)^{\frac{1}{2}} (f(\eta) + \eta f'(\eta) + g(\eta) + \eta g'(\eta)) \exp\left(\frac{x+y}{2}\right), \tag{14}$$

and the resulting dimensionless equations are

$$A_1 f''' + K g' + 2Gr\Theta - 2Mf' + f''(f+g) - 2f'(f'+g') = 0 \tag{15}$$

$$A_1 g''' - K f' + 2Gr\Theta - 2Mg' + g''(f+g) - 2g'(f'+g') = 0 \tag{16}$$

$$\left(1 + \frac{4}{3}R\right) A_2 \Theta'' + Pr(f+g)\Theta' - 4Pr\Theta(f'+g') + N_b \Theta'\Phi' + N_t \Theta'\Theta' = 0 \tag{17}$$

$$\Phi'' + \frac{N_t}{N_b}\Theta'' - Sc(4\Phi(f'+g') - \Phi'(f+g)) = 0 \tag{18}$$

with

$$f+g = 0, \ f' = 1, \ g' = \gamma, \ \Theta = 1, \ \Phi = 1, \quad \text{at } \eta = 0 \tag{19}$$

$$f' = 0, \ g' = 0, \ \Theta = 0, \ \Phi = 0, \quad \text{as } \eta \to \infty. \tag{20}$$

where

$$Gr = \frac{g\beta T_0}{U_0^2}, \ M = \frac{\sigma_{hnf} B_0^2}{\rho_{hnf} U_0}, \ Pr = \frac{\nu_{bf}}{\alpha_{bf}}, \ R = \frac{4\sigma^* T_\infty^3}{\alpha_{hnf} k^* (\rho c_p)_{hnf}}, \ K = \frac{4\Omega}{U_0 e^{x+y}}, Sc = \frac{\nu_{bf}}{D_B} \tag{21}$$

$$A_2 = \frac{(1+2\phi)(\phi_1 k_1 + \phi_2 k_2) + 2(1-\phi)\phi k_{bf}}{(1-\phi)(\phi_1 k_1 + \phi_2 k_2) + (2+\phi)\phi k_{bf}} \left(1 - \phi + \phi_1 \frac{(\rho c_p)_1}{(\rho c_p)_{bf}} + \phi_2 \frac{(\rho c_p)_2}{(\rho c_p)_{bf}}\right)^{-1}, \tag{22}$$

$$A_1 = \left(1 - \phi + \frac{\phi_1 \rho_1}{\rho_{bf}} + \frac{\phi_2 \rho_2}{\rho_{bf}}\right)^{-1} (1-\phi)^{-2.5}, N_b = \frac{\tau D_B}{\alpha_{bf}} e^{2x+2y}, N_t = \frac{\tau D_T}{\alpha_{bf} T_\infty} e^{2x+2y}, \gamma = \frac{V_0}{U_0}. \tag{23}$$

The system of equations (15 - 17) with the boundary and initial conditions are reformulated as a system of first order ordinary differential equations by setting

$$H_1 = f, H_2 = f', H_3 = f'', H_4 = g, H_5 = g', H_6 = g'', H_7 = \Theta, H_8 = \Theta', H_9 = \Phi, H_{10} = \Phi'$$

to give

$$\frac{d}{d\eta}H_1 = H_2, \quad \frac{d}{d\eta}H_2 = H_3, \tag{24}$$

$$\frac{d}{d\eta}H_3 = -\frac{1}{A_1}\left(KH_5 + 2GrH_7 - 2MH_2 + H_3\left(H_1 + H_4\right) - 2H_2\left(H_2 + H_5\right)\right), \tag{25}$$

$$\frac{d}{d\eta}H_4 = H_5, \quad \frac{d}{d\eta}H_5 = H_6, \tag{26}$$

$$\frac{d}{d\eta}H_6 = -\frac{1}{A_1}\left(-KH_2 + 2GrH_7 - 2MH_5 + H_6\left(H_1 + H_4\right) - 2H_5\left(H_2 + H_5\right)\right), \tag{27}$$

$$\frac{d}{d\eta}H_7 = H_8, \tag{28}$$

$$\frac{d}{d\eta}H_8 = -\left(\left(1 + \frac{4}{3}R\right)A_2\right)^{-1}\left(Pr\left(H_1 + H_4\right)H_8 - 4PrH_7\left(H_2 + H_5\right) + N_bH_8H_{10} + N_tH_8^2\right), \tag{29}$$

$$\frac{d}{d\eta}H_9 = H_{10}, \quad \frac{d}{d\eta}H_{10} = -\left(\frac{N_t}{N_b}\frac{d}{d\eta}H_8 - Sc\left(4H_9\left(H_2 + H_5\right) - H_{10}\left(H_1 + H_4\right)\right)\right), \tag{30}$$

with the initial conditions

$$H_1(0) = f_w,\ H_2(0) = 1,\ H_3(0) = s_1,\ H_4(0) = -f_w,\ H_5(0) = \gamma,$$
$$H_6(0) = s_2,\ H_7(0) = 1,\ H_8(0) = s_3, H_9(0) = 1, H_{10}(0) = s_4$$

and s_1, s_2, s_3, s_4 are chosen to satisfy the boundary conditions

$$H_2(\eta_\infty) = 0,\ H_5(\eta_\infty) = 0,\ H_7(\eta_\infty) = 0,\ H_9(\eta_\infty) = 0.$$

The equations (24 - 30) is solved using the bvp4c solver which executes the finite difference code that implements the three stage Lobatto IIIa formula of fourth order [17, 18]. The system is solved with absolute tolerance of 10^{-8} and relative tolerance of 10^{-8}. The thermophysical properties are listed out in table (1).

	c_p	ρ	k
Ethylene-Glycol	4179	997.1	0.613
Copper	385	8933	400
Alumina	765	3970	40

Table 1: thermophysical properties

Discussion of Results

Figures (2 - 5) depict the effects of Coriolis force on the Couette flow of Hybrid nanofluid over an exponentially stretching surface. Rotation of the surface gives rise to the Coriolis effect, which removes kinetic energy from the secondary motion and adds it to the primary motion. The flow is enhanced in the primary direction (see figure (2)) but the reduced in the secondary direction (see figure (3)). The additional kinetic energy introduced into the system raises the temperature. This explains why the temperature profiles increase as the Coriolis force increases in figure (4). As the rotation increases, the solutal boundary layer increases and hence, an increase in the concentration is expected as shown in figure (5). The flow under consideration is the Couette flow, which means that upper plate and the lower plate are moving independent of each other. The stretching ratio γ measures the rate at which the upper plate is moving relative to the lower plate. For $0 < \gamma < 1$, the lower plate is moving faster than the upper plate, while the upper plate is moving faster than the lower plate for $\gamma > 1$. The case $\gamma = 1$ represents the case where the upper and the lower plates move at the same rate. Figures (6 - 9)

show the effects of stretching ratio on the flow. Figure (6) shows that the primary velocity decreases when the upper plate stretches faster than the lower plate. This is due to the fact that fluid particles closest to the plates move at same speed with the plate. However, increasing the speed of the upper plate has a dual effect on the secondary velocity. Secondary velocity at the boundary layer increases as the stretching ratio increases, whereas the behaviour changes for the free stream (see figure (7)). Figures (8) and (9) show that the temperature and concentration are reduced with increasing stretching ratio.

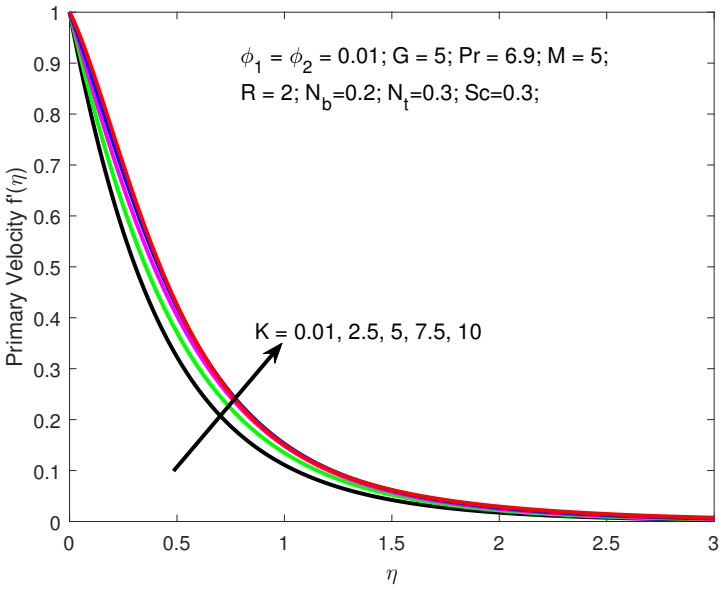

Figure 2: Coriolis effect on primary velocity

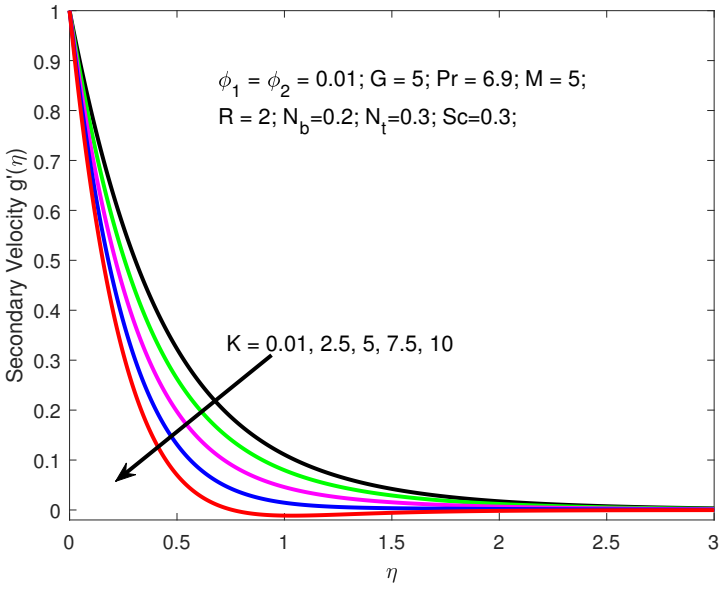

Figure 3: Coriolis effect on secondary velocity

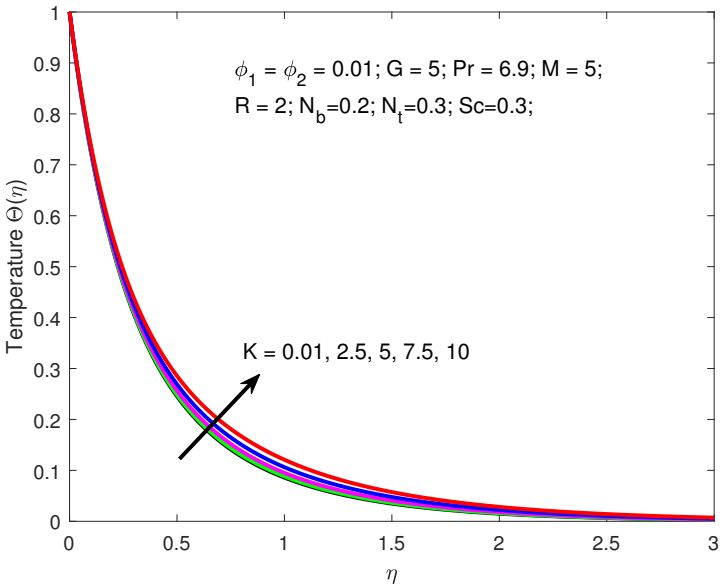

Figure 4: Coriolis effect on temperature

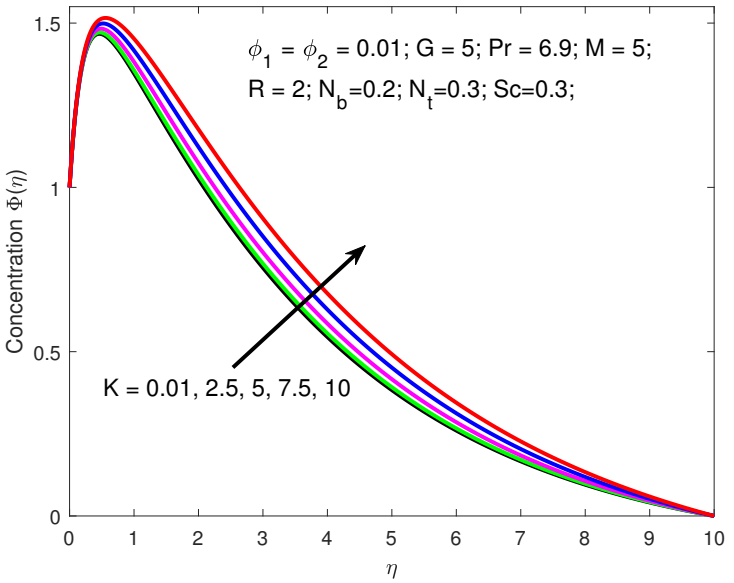

Figure 5: Coriolis effect on concentration

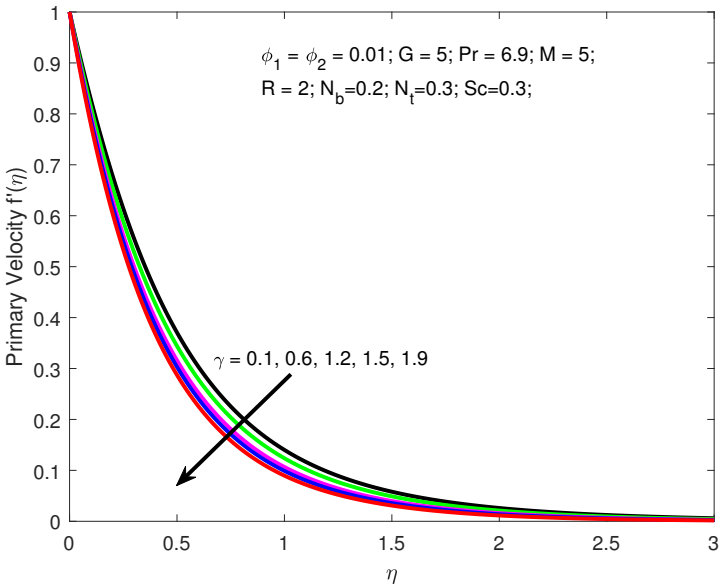

Figure 6: Effect of Stretching ratio on primary velocity

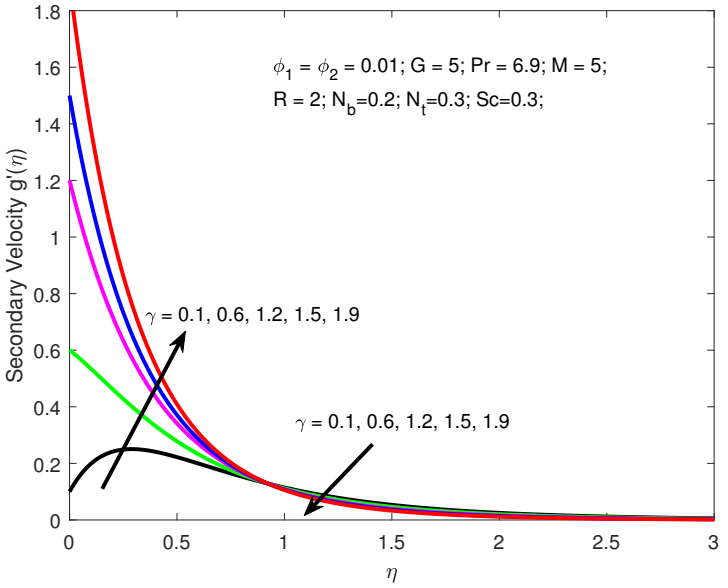

Figure 7: Effect of Stretching ratio on secondary velocity

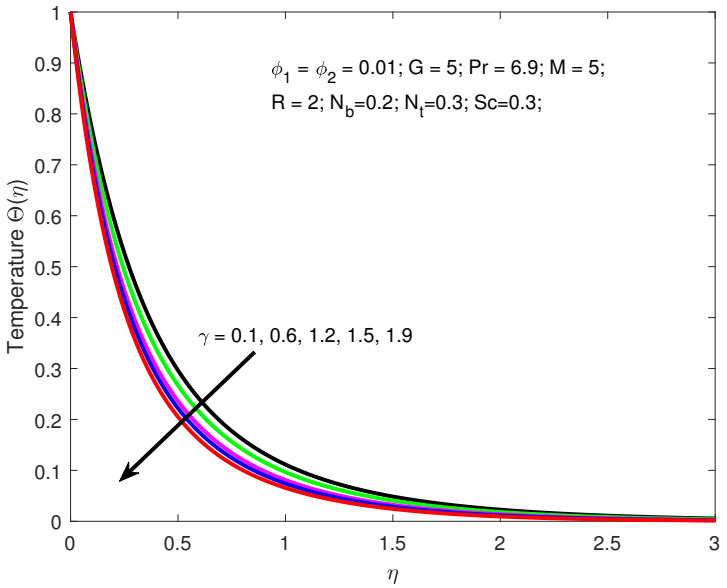

Figure 8: Effect of Stretching ratio on temperature

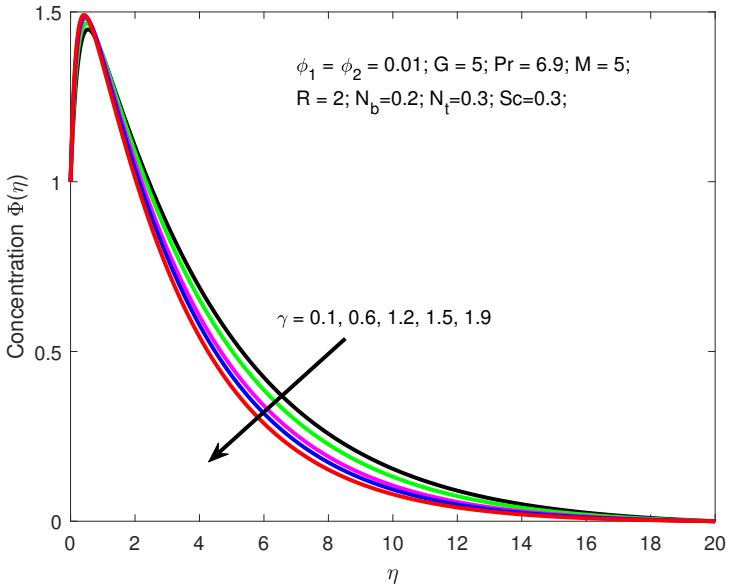

Figure 9: Effect of Stretching ratio on concentration

Conclusion

The flow of a hybrid nanofluid between two moving plates under the action of Coriolis force is analysed in this study. The governing equations are rendered dimensionless and the resulting ODE is solved using MATLAB bvp4c. The results show that

1. Coriolis force increases primary velocity but the reduces secondary velocity.

2. Coriolis force increases increases both the temperature and the concentration.

3. Raising the stretching ratio decreases primary velocity.

4. Raising the stretching ratio increases the secondary velocity in the boundary layer but increases it in the free stream.

5. Raising the stretching ratio reduces temperature and concentration.

References

[1] S. U. S. Choi, J. A. Eastman, Enhancing Thermal Conductivity of Fluids with Nanoparticles, ASME International Mechanical Engineering Congress & Exposition (1995).

[2] S. Suresh, K. P. Venkitaraj, P. Selvakumar, M. Chandrasekar, Effect of Al2O3–Cu/water hybrid nanofluid in heat transfer, Exper. Therm. Fluid Sci. 38 (2012), 54–60.

[3] J. O. Ouru, W. N. Mutuku, A. S. Oke, Buoyancy-Induced MHD Stagnation Point Flow of Williamson Fluid with Thermal Radiation, J. Eng. Res. Rep. (2020) 9–18

[4] A. S. Oke, W. N. Mutuku, Significance of viscous dissipation on MHD Eyring-Powell flow past a convectively heated stretching sheet, Pramana. 95 (2021), 199.

[5] A. S. Oke, Coriolis effects on MHD flow of MEP fluid over a non-uniform surface in the presence of thermal radiation, Int. Commun. Heat Mass Transfer 129 (2021), 105695.

[6] O. K. Koriko, K. S. Adegbie, A. S. Oke, I. L. Animasaun, Exploration of Coriolis force on motion of air over the upper horizontal surface of a paraboloid of revolution, Phys. Scripta 95 (2020), 035210.

[7] A. S. Oke, W. N. Mutuku, M. Kimathi, I. L. Animasaun, Insight into the dynamics of non-Newtonian Casson fluid over a rotating non-uniform surface subject to Coriolis force, Nonlinear Eng. 9 (2020), 398-411.

[8] A. S. Oke, W. N. Mutuku, M. Kimathi, I. L. Animasaun, Coriolis effects on MHD newtonian flow over a rotating non-uniform surface, Proc. Inst. Mech. Eng. Part C: J. Mech. Eng. Sci. 235 (2020), 3875-3887.

[9] B. Ali, Y. Nie, S. Hussain, D. Habib, S. Abdal, Insight into the dynamics of fluid conveying tiny particles over a rotating surface subject to Cattaneo-Christov heat transfer, Coriolis force, and Arrhenius activation energy, Comput. Math. Appl. 93 (2021), 130-143.

[10] B. A. Juma, A. S. Oke, W. N. Mutuku, A. G. Ariwayo, O. J. Ouru, Dynamics of Williamson fluid over an inclined surface subject to Coriolis and Lorentz forces, Eng. Appl. Sci. Lett. 5 (2022), 37-46.

[11] A.S. Oke, Combined effects of Coriolis force and nanoparticle properties on the dynamics of gold-water nanofluid across nonuniform surface, Z. Angew. Math. Mech. (2022). https://doi.org/10.1002/zamm.202100113.

[12] N. S. Anuar, N. Bachok, I. Pop, Cu-Al2O3/Water hybrid nanofluid stagnation point flow past MHD stretching/shrinking sheet in presence of homogeneous-heterogeneous and convective boundary conditions, Mathematics. 8 (2020), 1237.

[13] B. Takabi, S. Salehi, Augmentation of the heat transfer performance of a sinusoidal corrugated enclosure by employing hybrid nanofluid, Adv. Mech. Eng. 6 (2014), 147059.

[14] I. Tlili, H. A. Nabwey, G. P. Ashwinkumar, N. Sandeep, 3-D magnetohydrodynamic AA7072-AA7075/methanol hybrid nanofluid flow above an uneven thickness surface with slip effect, Sci. Rep. 10 (2020), 4265.

[15] I. Tlili, H. A. Nabwey, M. G. Reddy, N. Sandeep, M. Pasupula, Effect of resistive heating on incessantly poignant thin needle in magnetohydrodynamic Sakiadis hybrid nanofluid, Ain Shams Eng. J. 12 (2021), 1025–1032.

[16] A.S. Oke, I.L. Animasaun, W.N. Mutuku, M. Kimathi, N.A. Shah, S. Saleem, Significance of Coriolis force, volume fraction, and heat source/sink on the dynamics of water conveying 47 nm alumina nanoparticles over a uniform surface, Chinese J. Phys. 71 (2021), 716-727.

[17] L. F. Shampine, M. W. Reichelt, J. Kierzenka, Solving Boundary Value Problems for Ordinary Differential Equations in MATLAB with bvp4c. (2010).

[18] A. S. Oke, Convergence of Differential Transform Method for Ordinary Differential Equations, J. Adv. Math. Comput. Sci. 24 (2017), 1-17.

Nomenclature			
x, y, z	Distance in three dimensional space	ϕ	overall nanoparticle volume fraction
u, v, w	Velocity component in the x, y, z-directions	ϕ_1	volume fraction of Cu nanoparticle
T	Dimensional fluid temperature	ϕ_2	volume fraction of Al_2O_3 nanoparticle
T_w	wall temperature	k_{hnf}	effective hybrid nanofluid thermal conductivity
T_∞	free stream temperature	k_{bf}	thermal conductivity of base fluid
B_0	magnetic field strength	k_1	thermal conductivity of Cu nanoparticle
γ	angle of inclination of magnetic field	k_2	thermal conductivity of Al_2O_3 nanoparticle
K	rotation parameter	k^*	mean absorption coefficient
Gr	Grashof number	σ_{hnf}	effective electrical conductivity of hybrid nanofluid
M	Magnetic field parameter	α_{hnf}	effective hybrid nanofluid thermal diffusivity
R	thermal radiation parameter	α_{bf}	thermal diffusivity of base fluid
Pr	Prandtl number	g^*	Acceleration due to gravity
ρ_{hnf}	effective hybrid nanofluid density	μ_{hnf}	effective hybrid nanofluid viscosity
ρ_{bf}	base fluid density	μ_{bf}	base fluid viscosity
ρ_1	nanoparticle density of Cu nanoparticle	σ^*	Stefan–Boltzmann constant
ρ_2	nanoparticle density of Al_2O_3 nanoparticle	$(c_p)_{hnf}$	effective Specific heat capacity of hybrid nanofluid
Ω	angular velocity of the surface	$(c_p)_{bf}$	Specific heat capacity of the base fluid
β	Coefficient of thermal expansion	$(c_p)_1$	Specific heat capacity of Cu nanoparticle
ν_{bf}	kinematic viscosity of base fluid	$(c_p)_2$	Specific heat capacity of Al_2O_3 nanoparticle
D_T	Thermophoretic diffusion coefficient	D_B	Brownian diffusivity